Journal of Hazardous Materials 171 (2009) 358–369

Contents lists available at ScienceDirect

Journal of Hazardous Materials

journal homepage: www.elsevier.com/locate/jhazmat

A preliminary study on the adsorptive removal of Cr(VI) using seaweed, *Hydrilla verticillata*

S.S. Baral[a,*], Namrata Das[b], G. Roy Chaudhury[b], S.N. Das[b]

[a] *Chemical Engineering Group, Birla Institute of Technology & Science, Pilani – Goa Campus, Zuarinagar, Goa-403726, India*
[b] *Department of Environment and Sustainability, Institute of Minerals and Materials Technology, Bhubaneswar-751013, India*

ARTICLE INFO

Article history:
Received 15 March 2009
Received in revised form 13 May 2009
Accepted 4 June 2009
Available online 11 June 2009

Keywords:
Cr(VI) adsorption
Seaweed
Factorial design
Mechanism
Thermodynamics
Multivariate analysis

ABSTRACT

The Cr(VI) adsorption efficiency of the seaweed, *Hydrilla verticillata*, was studied in batches. The adsorbent was characterized using SEM, BET surface area analyzer, Malvern particle size analyzer, EDAX and FT-IR. Cr(VI) removal efficiency of the adsorbent was studied as a function of different adsorption parameters such as contact time, stirring speed, pH, adsorbent dose, particle size, adsorbate concentration, and temperature. Langmuir, Freundlich, and Temkin adsorption isotherm equations were used in the equilibrium modeling. The adsorption process followed pseudo second-order kinetics and intra-particle diffusion was found to be the rate-controlling step. Experimental data follow Langmuir adsorption isotherm. Thermodynamic parameters such as Gibbs free energy and enthalpy of the adsorption process were evaluated to find out the feasibility of the adsorption process. The negative values of Gibb's free energy and positive enthalpy values show the feasibility and endothermic nature of the process. The significance of different adsorption parameters along with their combined effect on the adsorption process has been established through a full 2^4 factorial design. Among the different adsorption parameters, pH has the most influential effect on the adsorption process followed by adsorbate concentration and combined effects of all the four parameters were tested. The correlation among different adsorption parameters were studied using multi-variate analysis.

1. Introduction

Contamination of water by traces of heavy metal ions has been paid increasing attention by people all over the world. Among the various heavy metals, Cr(VI) is highly toxic for living organisms [1,2]. While hexavalent and trivalent species of chromium are prevalent in industrial and mining wastewater, the hexavalent form has been considered more hazardous to living organisms due to its mutagenic and carcinogenic properties [3,4]. Its smaller size as compared to Cr(III), high mobility and high oxidizing potential makes Cr(VI) more toxic for living organisms. Especially, in presence of ascorbic acid, it tends to modify the cell DNA causing abnormality in cell growth and ultimately cancer. The permissible limit of Cr(VI) in potable water is 0.05 mg/L [5] while that of industrial discharges are allowed to go up to 0.2 mg/L. But the industrial and mining effluents contain much higher concentrations compared to the permissible limit. Thus, the treatment of wastewater to reduce/remove Cr(VI) before discharging into the environment, is inevitable [6].

There are different methods used for the treatment of Cr(VI) contaminated water including ion exchange [7], membrane separation [8], electrolytic reduction [9], solvent extraction [10], chemical reduction followed by precipitation [11], etc. However, these processes have a number of disadvantages like incomplete metal removal, high cost and producing toxic chemical sludge or disposal of other waste products [12,13]. Among other processes for removal of Cr(VI) from industrial/mining wastewater, adsorption process is a potential and economically feasible alternative [14]. In recent years, increased attention has been focused on the use of naturally available low cost biomaterials for the treatment of Cr(VI) contaminated water [15]. Heavy metal adsorption using biomaterials can reduce capital cost by 20%, operational cost by 36%, and total treatment cost by 28%, as compared to other treatment processes [16]. Use of biomaterials even makes the adsorption process more environment friendly and more technically feasible. Further, biomaterials can retain/reduce relatively high quantities of Cr(VI) ions by adsorption and/or complexation [17,18].

A survey of literature shows that though tremendous efforts are continuing world wide to improvise low cost adsorbents having high loading capacities, it remains an area of intensive R&D. Out of the various adsorbents used, many adsorbents have very low adsorption capacity. Some adsorbents have very high adsorption capacity but at a relatively lower pH. Again the treatment of adsorbents in some cases may not be cost effective. Considering the above facts, a new low cost adsorbent i.e., *Hydrilla*

* Corresponding author. Tel.: +91 9767022314.
E-mail address: ss_baral2003@yahoo.co.in (S.S. Baral).

0304-3894/$ – see front matter © 2009 Elsevier B.V. All rights reserved.
doi:10.1016/j.jhazmat.2009.06.011

verticillata was used in the present study to treat Cr(VI) contaminated wastewater. Batch adsorption experiments were carried out to find the adsorption kinetics, mechanism and optimum Cr(VI) loading capacity of the adsorbent. Different mathematical models such as adsorption kinetics, adsorption isotherm and mass transfer models were applied to the experimental data to find out the best fit. Statistical design of the experiment was used to find out the most influential parameters along with their combined effect.

2. Materials and method

2.1. Materials

The biosorbent *H. verticillata* (local name: Chingudia Dala) used in this study was collected from Nairipentha side of Chilka, a semi-saline waterbody situated at a distance of ~90 km from Bhubaneswar, the capital city of Orissa. *Hydrilla verticillata* is a waste weed which grows profusely in the semi-saline water. Chilka has a water span of 850–1000 km^2. The weed is present all over the semi-saline portion (750 km^2) barring the seaside of the lake. It grows during dry season (October–June) and gets totally submerged during monsoons when the water level rises during which a part of the weed population perishes adding carbon to the silt. The collected seaweed was washed thrice with tap water and four times with deionized water. The washed biomass was dried in sunlight for 5 days followed by drying in an oven at 60 °C for 24 h. The resulting dried seaweed was crushed in a mill, sieved to different size fractions and stored in polyethylene bottles until use.

2.2. Method

The stock Cr(VI) solution having concentration 1000 mg/L was prepared by using $K_2Cr_2O_7$ (analytical grade). Experimental solutions of the desired concentrations were obtained by successive dilution. The pH of the solution was maintained at desired value by adding dilute HCl or NaOH solution before adsorption. All experiments were carried out using AR/GR grade E Merck chemicals. Adsorption experiments were carried out in 500-mL volumetric flask using 250 mL Cr(VI) solution with required amount of adsorbent. The mixtures were agitated by a Remi make mechanical stirrer with speed regulator. Adsorption studies were carried out at different temperatures using an automatic temperature controlled water bath with an accuracy of ±1 °C. For higher temperatures, the adsorption studies were carried out in a sealed unit to avoid loss due to evaporation. 5 mL of the samples were drawn and filtered at regular intervals. The mixture was filtered through Whatman 42 filter paper. The residual Cr(VI) concentration in the filtrate was determined by diphenylcarbazide method, using an UV/Visible Spectrophotometer (PerkinElmer Lambda-35) [19]. All the experiments were performed in triplicate and the average of three was taken for subsequent calculations. The difference between duplicate experimental values was in the range of ±3%.

3. Results and discussion

3.1. Characterization of adsorbent

Analysis by Malvern particle size analyzer (model 2000) showed the average particle size of the adsorbent to be 53.4 μm. The specific surface area of the powder was analyzed by nitrogen adsorption at 77 K applying BET method in Quantasorb (Quanta Chrom-USA). Degassing at 100 °C and 2–10 mm Hg for 2 h was performed prior to the measurement. The physico-chemical characteristics of the adsorbent are given in Table 1. SEM analysis (SEM JXO-8100) at 300× magnification was undertaken to find out the change in morphology after adsorption. The SEM images for the seaweed before and after adsorption are shown in Figs. 1 and 2 respectively. It shows irregular surface initially which turned smooth after adsorption. It is clearly observed that the pores and surfaces of the adsorbent were covered by Cr(VI) molecules and became smooth after adsorption. Further, adsorption of Cr(VI) on the surface of the adsorbent was confirmed from the elemental analysis by EDAX method. The EDAX images for the seaweed before and after adsorption are shown in Figs. 3 and 4. From the EDAX analysis, the mass percentage of the chromium on the adsorbent surface before and after adsorption was found to be 0.54 and 40.97% respectively. The higher mass per-

Table 1
Physical properties of the seaweed *Hydrilla verticillata*.

Parameters	Value
Specific gravity	0.65
Bulk density (g/cc)	0.55
Porosity (%)	74
Surface area (m^2/g)	30.9
Average particle size	97.6 μm
Moisture content (%)	63
Loss on ignition	95.4 (w/w, %)
Al_2O_3	1.5 (w/w, %)
SiO_2	1.3 (w/w, %)
FeO_2	0.22 (w/w, %)

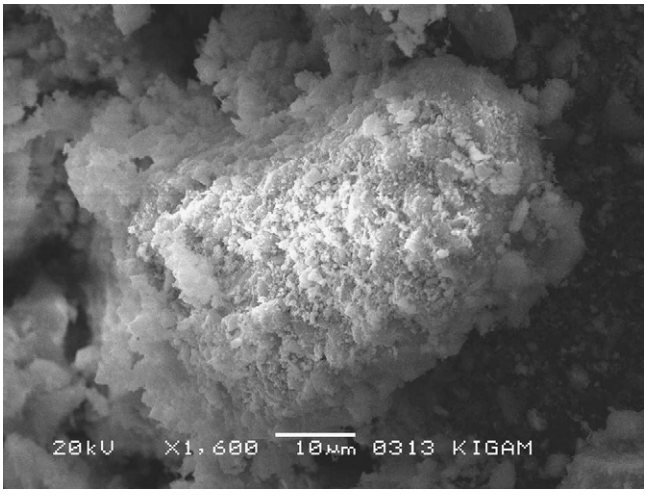

Fig. 1. SEM image of seaweed before adsorption.

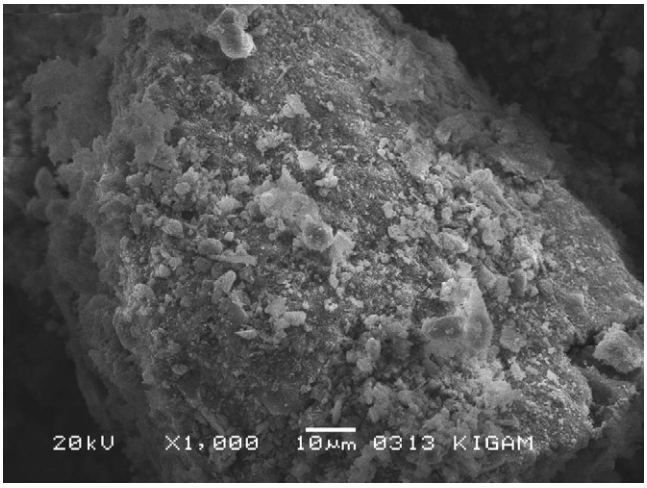

Fig. 2. SEM image of seaweed after adsorption.

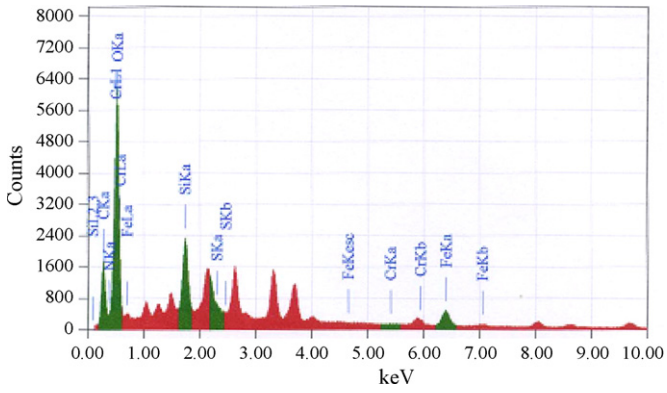

Fig. 3. EDAX image of seaweed before adsorption.

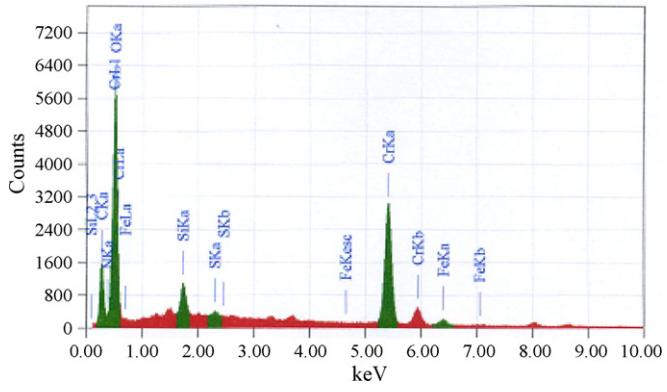

Fig. 4. EDAX image of seaweed after adsorption.

centage of chromium in the used adsorbent clearly indicates the adsorption of Cr(VI) on the surface of the adsorbent.

The FT-IR spectra of the seaweed, before and after adsorption of chromium were used to determine the vibrational frequency changes in the functional groups of the adsorbents. Infrared absorption spectra of the adsorbent before and after adsorption were obtained using a JASCO FTIR-3500 spectrometer. The samples were ground with 200 mg of KBr (spectroscopic grade) in a mortar and pressed into 10 mm diameter disks at 10 tons of pressure and high vacuum for FTIR analysis. The conditions used were 16 scans at a resolution of 4 cm^{-1} measured between 600 and 4000 cm^{-1}. The FT-IR spectra of the adsorbents display a number of absorption peaks, indicating the complex nature of the studied adsorbents. Table 2 presents the fundamental peaks of the adsorbents before and after use. In the seaweed before adsorption, the absorption peak around 3430 cm^{-1} can be assigned to stretching vibration of OH and NH stretching. The peaks observed at 3330 cm^{-1} indicate the H bond and OH group. The peaks around 2920 cm^{-1} correspond to the CH_2 asymmetric stretching vibration. The peak at 1740 cm^{-1} can be assigned to C=O stretching. The broad band absorption peak observed at 1570 cm^{-1} indicates the presence of secondary amino group. The other absorbance bands for the seaweed as such showed three sharp peaks at 1550 cm^{-1} (amide bonds), 1415 cm^{-1} (C–O stretching) and 1370 cm^{-1} (carboxyl group); one broad band at 1035 cm^{-1} (C–O stretching and SiO stretching) and a small peak at 875 cm^{-1} (aromatic CH). It is observed from Table 2 that the Cr(VI) adsorbed seaweed showed either a shift or reduction in absorption peak, suggesting the vital role played by the functional groups. These band shifts indicate that the bonded –OH groups and/or –NH stretching and carboxyl groups especially play a major role in Cr(VI) biosorption on seaweed. Similar observations related to Cr(VI) adsorption were observed by other researchers [20,6].

Table 2
The FT-IR spectral characteristics of seaweed before and after adsorption.

IR peak	Adsorption band (cm^{-1})		Difference	Assignment
	Before adsorption	After adsorption		
1	3430	3444	14	OH and NH stretching
2	2920	–	–	CH_2 asymmetric stretching vibration
3	1740	1734	−6	C=O stretching
4	1672	1679	7	C=O stretching
5	1570	1580	10	Secondary amine group
6	1553	1559	6	Amide bond
7	1415	1420	5	C=O stretching
8	1367	1379	12	Carboxyl group
9	1034	1330	−4	C=O and SiO stretching
10	875	881	6	Aromatic CH

3.2. *Effect of stirring speed*

Adsorption of Cr(VI) on the surface of the adsorbent is governed by the four consecutive steps [21]:

- Transport of adsorbate in the bulk solution.
- Diffusion of adsorbate across the liquid film boundary surrounding the adsorbent particle.
- Intra-particle diffusion of the adsorbate in the pores of the adsorbent.
- Sorption and desorption within the particle and on the external surface.

Among the above four steps, external transport, i.e., transport in the bulk solution and film diffusion is usually the rate limiting steps because of the poor mixing of the adsorbent particles in the solution. In order to find out the optimum stirring speed at which the external resistance to the mass transfer played insignificant role, adsorption experiments were carried out by varying the stirring speed. Cr(VI) adsorption studies were carried out by varying the agitation speed from 200 to 800 rpm and the results are shown in Fig. 5. The percentage of adsorption and the loading capacity of the adsorbent were found to be increase from 60 to 80.1 and 30 to 40.05 mg/g respectively when the stirring speed increased from 200 to 600 rpm. Thereafter, the adsorption process attained a steady state. The increase in Cr(VI) adsorption capacity of the adsorbent may be due to reduced film resistance to the adsorbent and slightly distorted the adsorbent structure at higher stirring speed. Under these experimental conditions, it can be safely assumed that

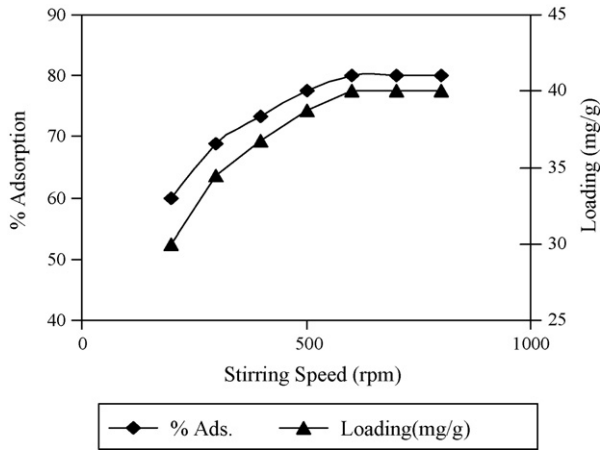

Fig. 5. Effect of stirring speed (conditions: pH 3.0; adsorbent dose 2 g/L; adsorbate concentration 100 mg/L; temperature 27 °C).

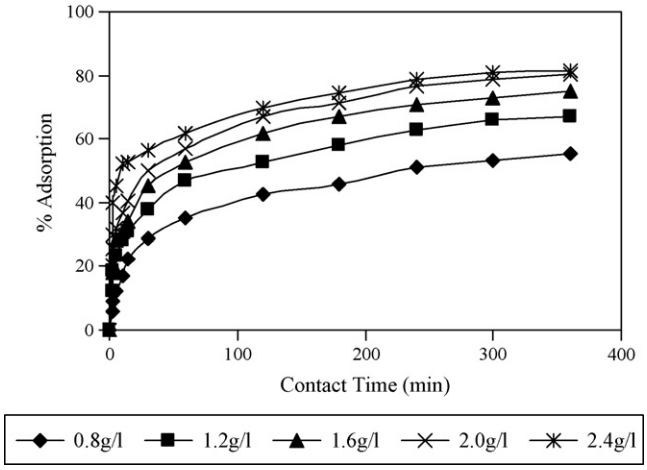

Fig. 6. Effect of contact time (conditions: pH 3.0; stirring speed 600 rpm; adsorbate concentration 100 mg/L; temperature 27 °C).

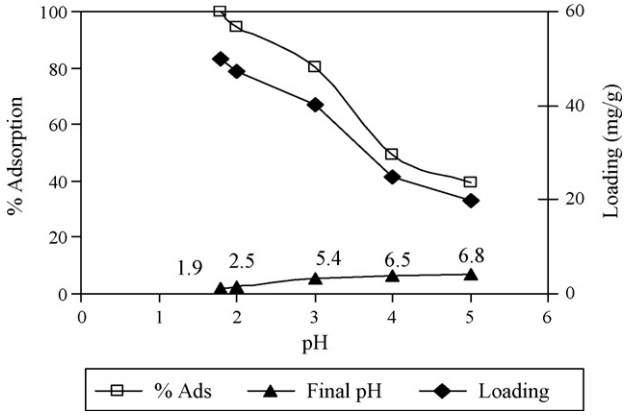

Fig. 7. Effect of pH (conditions: stirring speed 600 rpm; adsorbent dose 2 g/L; adsorbate concentration 100 mg/L; temperature 27 °C).

the solution homogeneity can be maintained and there may be no appreciable attrition of the adsorbent particle during the adsorption process. As 600 rpm was found to be the optimum stirring speed, the rest of the experiments were carried out at this stirring speed.

3.3. Effect of contact time

Adsorption experiments were carried out over 900 min to find the equilibrium contact time. During the experiment, the other adsorption parameters such as stirring speed, adsorbent dose, adsorbate concentration, pH and temperature of the solution were kept constant at 600 rpm, 2 g/L, 100 mg/L, 3.0 and 27 °C, respectively. The results are shown in Fig. 6. It can be seen from the figure that the kinetics was very fast during the first 30 min followed by a slower kinetics. During the faster phase, 70% of the total adsorption was reached. The adsorption process attained equilibrium within 6 h and beyond that, there was hardly any change in concentration. Therefore, all further studies were carried out for 6 h. The initial faster rate may be due to the higher free surface available initially. Once the available free surface is clogged, then the adsorbate molecules penetrate through the pores and get adsorbed inside the pore, which is known as intra-particle diffusion. The intra-particle diffusion accounts for the slower kinetics at the later stage. Similar dual mechanisms are also reported by others [22].

3.4. Effect of pH

Earlier studies on biosorption of Cr(VI) showed that pH is an important parameter affecting the adsorption process [23–26]. Adsorption experiments were carried out by varying the pH between 1.8 and 5.0 to find out its effect on the percentage of adsorption and Cr(VI) uptake capacity of the adsorbent. The results are shown in Fig. 7. It was observed that the maximum adsorption occurred at pH 1.8. The sorption capacity of Cr(VI) at pH 1.8 by the seaweed was 50 mg/g, which came down to 19.8 mg/g at pH 5. The optimum pH for the Cr(VI) adsorption process was found to be 1.8. But this lower pH (1.8) of the effluent water in the process needs another acid neutralization step which may not be economical. Therefore further adsorption studies were carried out at pH 3.

The mechanism by which metal ions are adsorbed onto the surface of the adsorbent has been a matter of considerable debate. Theories including ion exchange, surface adsorption, chemisorption, complexation, adsorption–complexation and adsorption–reduction were reported in the literature. Opinions differ as to how complexation occurs between adsorbent and Cr(VI) ions. Evidence has also been found that chemisorption, a strong type of adsorption in which ions are not exchanged but electrons may be exchanged, can be involved in biomaterial–metal binding [27]. Different mechanisms, such as electrostatic forces, ion exchange, and chemical complexation, must be taken into account while examining the effect of pH on Cr(VI) sorption. One of the commonly proposed mechanisms is electrostatic attraction/repulsion between adsorbent and adsorbate. Many studies have claimed that Cr(VI) was removed from the aqueous phase through an adsorption mechanism, whereby anionic Cr(VI) ion species bind to the positively charged groups of non-living biomass [23,28,29]. Cr(VI) was completely reduced to Cr(III) in contact with biomass [23,30].

Cr(VI) can be removed from the aqueous phase by non-living biomass through two mechanisms i.e., direct reduction and indirect reduction mechanisms. Cr(VI) is directly reduced to Cr(III) in the aqueous phase by contact with the electron-donor groups of the biomass, i.e., groups having lower reduction potential than that of Cr(VI). The indirect reduction consists of three steps: (1) binding of anionic Cr(VI) species to the positively charged groups present on the biomass surface, (2) reduction of Cr(VI) to Cr(III) by adjacent electron-donor groups followed by (3) release of Cr(III) ions into the aqueous phase due to electronic repulsion from the positively charged groups, or complexation of Cr(III) with adjacent groups capable of binding [30]. In the direct reduction mechanism, concentration of Cr(III) should increase with time. To find the possibility of direct reduction of Cr(VI) to Cr(III) in the solution during the adsorption process, the initial and final concentrations of Cr(III) in the solution were estimated using Atomic Absorption Spectrometer (AAS). It is found that there is hardly any change in Cr(III) concentration in the solution. Therefore, it can be concluded that Cr(VI) was not removed from the aqueous phase through direct reduction. Amino and carboxyl groups being electron donors are capable of affecting indirect reduction. As the pH of the aqueous phase is lowered, a large number of hydrogen ions can easily coordinate with the amino and carboxyl groups present on the biomass surface.

The proposed adsorption mechanism of Cr(VI) on the protonated amine groups of the seaweed is shown in Fig. 8. Thus, low pH makes the biomass surface more positively charged leading to faster removal rate of Cr(VI) in the aqueous phase since the binding of anionic Cr(VI) ion species to the positively charged groups is enhanced [29,30]. The low pH also accelerates the reduction reaction, since the protons take part in this reaction. Thus, the solution pH is the most important controlling parameter in the practical use of non-living biomass in the adsorption process [31]. Hence, lower pH of wastewater containing heavy metals is generally helpful in

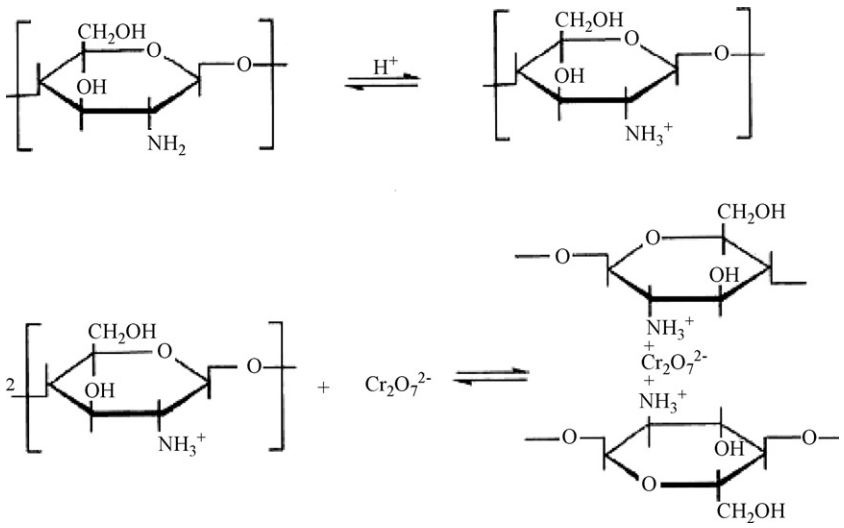

Fig. 8. Mechanism for Cr(VI) adsorption on seaweed. *Source*: Boddu et al. [54].

the process of adsorption over biomass. Meanwhile, if there are a small number of electron-donor groups in the biomass or protons in the aqueous phase, the chromium bound to the biomass can remain in the hexavalent state. Therefore, the adsorption mechanism depends on the biosorption parameters such as solution pH, temperature, biomass and Cr(VI) concentrations [30].

3.5. Effect of adsorbate concentration

Two different oxidation states (3+ and 6+) dominate Cr chemistry. Cr(VI) can be present in two different anionic forms: CrO_4^{2-} and $Cr_2O_7^{2-}$, which are sensitive to the pH of the medium. While CrO_4^{2-} is the dominating form in pH > 8, $Cr_2O_7^{2-}$ is usually found in the pH range 2–6. In still higher acidic conditions (pH < 1), it is converted to chromic acid ($H_2Cr_2O_7$). Since the present studies were carried out in the pH range 1.8–5.0, all the Cr can safely be assumed to be in $Cr_2O_7^{2-}$ form [32].

It can be seen from Fig. 9 that when the initial Cr(VI) concentration increased from 50 to 250 mg/L, Cr(VI) removal decreased from 100 to 44.6% and the Cr(VI) uptake capacity of the biomass increased from 25.0 to 55.8 mg/g. Probably higher concentration of Cr(VI) led to faster and more binding sites compared to lower initial Cr(VI) concentration at the same dose of adsorbent. Moreover, higher initial Cr(VI) concentration increased driving force to overcome the mass transfer resistance of metal ions between the aqueous and solid phases resulting in higher probability of collision between the adsorbates with adsorbents. This also results in higher metal uptake [33]. The increase of Cr(VI) loading capacity of the biomass with increasing initial Cr(VI) concentration may also be due to higher interaction between the metal ions and adsorbent. However, the seaweed offered a finite number of surface binding sites and Cr(VI) adsorption showed a saturation trend at higher initial Cr(VI) concentration.

3.6. Effect of adsorbent dose

Adsorption experiments were carried out to evaluate the effect of adsorbent dose on Cr(VI) removal. The trend of adsorption at varying doses of adsorbent is shown in Fig. 10. The percentage of Cr(VI) removal increased from 55.1 to 81.5 with increase in adsorbent dose from 0.8 to 2.4 g/L. The trend was as per expectations since more active sites of adsorbent were exposed when the adsorbent dose increased. However, the Cr(VI) uptake capacity of the adsorbent decreased from 68.9 to 33.7 mg/g when the adsorbent dose increased from 0.8 to 2.4 g/L. Further, it was observed that after rapid increase in percentage adsorption of Cr(VI) ions with increase in adsorbent dose up to 2.0 g/L, the rate of Cr(VI) removal attained an asymptotic value for larger doses of adsorbent. The sluggish rise in Cr(VI) removal beyond an optimum dose may be attributed to the

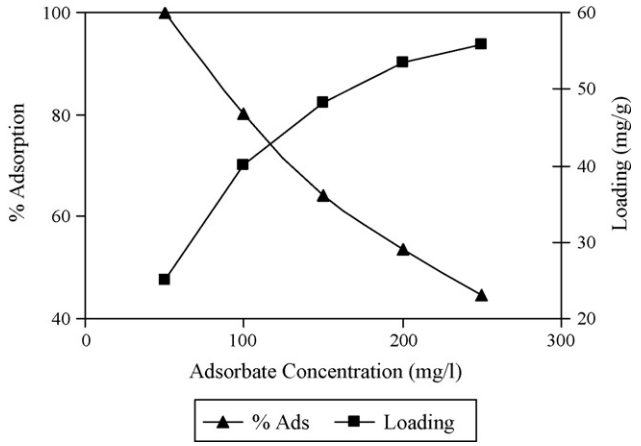

Fig. 9. Effect of adsorbate concentration (conditions: pH 3.0; adsorbent dose 2 g/L; stirring speed 600 rpm; temperature 27 °C).

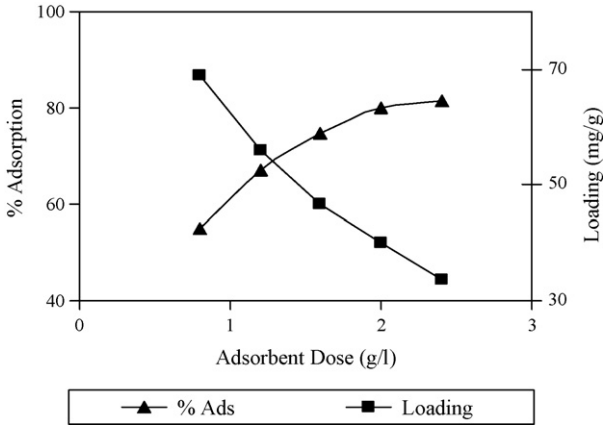

Fig. 10. Effect of adsorbent dose (conditions: pH 3.0; stirring speed 600 rpm; adsorbate concentration 100 mg/L; temperature 27 °C).

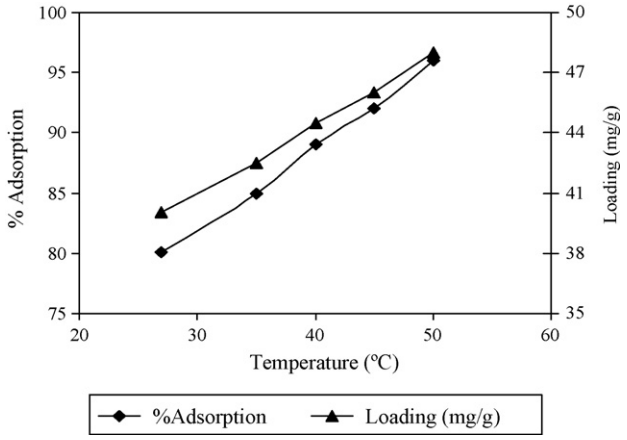

Fig. 11. Effect of temperature (conditions: pH 3.0; adsorbent dose 2 g/L; adsorbate concentration 100 mg/L; stirring speed 600 rpm).

attainment of equilibrium between adsorbate and adsorbent under the experimental conditions. This effect had been termed as "solid concentration effect", i.e., overcrowding of particles by Mehrotra et al. [34].

3.7. Effect of temperature

The effect of temperature on the percentage of adsorption and Cr(VI) uptake capacity of the adsorbent is presented in Fig. 11. It can be observed that the percentage of Cr(VI) adsorption increased from 80.1 to 96% when the temperature increased from 27 to 50 °C. Similarly, the uptake capacity of the adsorbent increased from 40.05 to 48 mg/g when the temperature increased from 27 to 50 °C. The increase in Cr(VI) uptake capacity may be attributed to the followings [33]:

- The increase in Cr(VI) adsorption capacity of the adsorbent with temperature indicates the endothermic nature of the adsorption process.
- The rise in sorption capacity with temperature is because of rise in the kinetic energy of adsorbent particles. In which case, the collision frequency between adsorbent and adsorbate increases resulting in enhanced sorption on to the surface of the adsorbent.
- Further, bond rupture of the functional groups on adsorbent surface at an elevated temperature may increase the number of active sorption sites, which may also lead to enhanced adsorption capacity of the adsorbent.
- The extent of protonation of the functional groups increases at higher temperatures resulting in an increase in the metal adsorption capacities at high temperature.

The effect of temperature on the equilibrium constant (K_C) of the adsorption of metal ions onto the seaweed was also investigated. Equilibrium constants for Cr(VI) increased as temperature increases and hence adsorption increased with temperature. The thermodynamic parameters such as standard Gibbs free energy change (ΔG^0), enthalpy change (ΔH^0) and entropy change (ΔS^0) were estimated to evaluate the feasibility and nature of the adsorption process [35]. The relationship between Gibb's free energy change to the equilibrium constant is given by the equation:

$$\Delta G^0 = -RT \ln K_C \quad (1)$$

$$K_C = \frac{C_a}{C_e} \quad (2)$$

where K_C = equilibrium constant; C_a = mg of adsorbate adsorbed per liter of adsorbent; C_e = equilibrium concentration of solution mg/L; T = absolute temperature; R = universal gas constant.

The values of Gibbs free energy decrease from −1.74 to −6.67 kJ/gmol when the temperature increases from 27 to 50 °C. The adsorption process is endothermic, hence the amount adsorbed at equilibrium must increase with increasing temperature, which explains increasingly negative ΔG^0 values with the rise in temperature. The carboxylic and amine groups of the seaweed are partially protonated at all temperatures but their degree of protonation increases at higher temperatures resulting in an increase in the metal adsorption capacities at high temperatures. The 'chelating effect' causes a large positive change in entropy, which means that the change of Gibbs free energy with temperature will be negative. Considering other thermodynamic factors, the entropy change in chelation reactions may have less bearing on temperature effects than the enthalpy of sorption. Thus, as the temperature increases, the resulting ΔG^0 will become more negative and so the equilibrium constant will increase slightly [36–40]. Assuming that the activity coefficients are unity at low concentrations (the Henry's law sense), thermodynamic parameters such as enthalpy change (ΔH^0) and entropy change (ΔS^0) were calculated using the following relations [41]:

$$\ln K_C = \frac{\Delta S^0}{R} - \frac{\Delta H^0}{RT} \quad (3)$$

The values of ΔH^0 and ΔS^0 were obtained from the linear Van't Hoff plot of $\ln K_C$ vs. $1/T$ from Eq. (3) and are found to be 59.9 and 0.204 J/gmol-K respectively. The positive values of ΔH^0 indicate the endothermic nature of the process while the negative ΔS^0 corresponds to a decrease in the degree of freedom of the adsorbed species [42]. The order of magnitude of the enthalpy change as well as the relatively slow rate of the adsorption suggests the adsorption to be of a chemical type. Similar results have been reported for the Cr(VI) adsorption onto activated carbon [43]. This may be attributed to a relative increase in adsorbing tendency of the solute from the adsorbent phase to the bulk phase with the rise in the temperature of the solution.

3.8. Adsorption kinetics study

The study of adsorption kinetics in wastewater is significant as it provides valuable insight into the reaction pathways and into the mechanism of the reaction. Further, it is important to predict the time at which the adsorbate is removed from aqueous solution in order to design an appropriate sorption treatment plant. Any adsorption process is normally controlled by three diffusive transport processes for the adsorbate:

- From bulk solution to the film surrounding the adsorbent.
- From the film to the adsorbent surface.
- From the surface to the internal sites followed by binding of the metal ions onto the active sites.

But in kinetic modeling, all these three steps are grouped together and it is assumed that the difference between the average solid phase concentration and equilibrium concentration is the driving force for adsorption. Further, it is established from the experimental observations that at optimum agitation speed, the external boundaries have hardly any effect. So application of the kinetic model depends only on the initial and final concentrations of the solution at different time intervals. Several kinetic models have been proposed to clarify the mechanism of a solute sorption from aqueous solution onto an adsorbent:

- Pseudo first-order/Lagergren kinetic model
- First-order reversible kinetic model
- Ritchie's second-order kinetic model
- Pseudo second-order kinetic model

3.8.1. Pseudo first-order or Lagergen kinetic model

The Pseudo first-order or Lagergen kinetic rate equation for the sorption of liquid–solid system was derived based on the adsorption capacity of the solid. It is one of the most widely used rate equations for sorption of a solute from a liquid solution. According to the authors, the overall adsorption rate is directly proportional to the driving force, i.e., the difference between initial and equilibrium concentrations of the adsorbate ($q_e - q$). Therefore, the pseudo first-order kinetic equation can be expressed as:

$$\frac{dq_e}{dt} = k(q_e - q) \tag{4}$$

where 'q_e' is the amount of solute adsorbed at equilibrium per unit mass of adsorbent (mg/g), 'q' is the amount of solute adsorbed at any given time 't' and 'k' is the rate constant. By using the boundary conditions and simplifying, Eq. (4) becomes

$$\log(q_e - q) = \log\, q_e - \frac{k}{2.303}t \tag{5}$$

The values of 'k' were calculated from the slope of the linear plot between $\log(q_e - q_t)$ and 't' for different adsorption parameters such as pH, temperature, adsorbate concentration, adsorbent dose and agitation speed. The correlation coefficients and rate constants are given in Table 3. The correlation coefficients were in good agreement with the pseudo first-order kinetics.

3.8.2. First-order reversible kinetic model

The sorption process may be considered as a first-order reversible reaction, which can be expressed as

$$A \underset{k_2}{\overset{K}{\rightleftharpoons}} B$$

The rate equation for the reaction is expressed as

$$\ln(1 - U_t) = -(k_1 + k_2)t, \tag{6}$$

where 'U_t' is the fractional attainment of equilibrium and is given by

$$U_t = \frac{C_{A0} - C_A}{C_{A0} - C_{Ae}} \tag{7}$$

where 'C_A' (mg/L) and 'C_B' (mg/g) are the concentrations of the adsorbate in solution and adsorbent respectively at a given time 't'; '$C_{A0}{}'$' and '$C_{B0}{}'$' are the initial concentrations of adsorbate and adsorbent respectively; '$k_1{}'$' and '$k_2{}'$' are the first-order rate constants. Under equilibrium conditions the following relations hold good:

$$K_C = \frac{C_{Be}}{C_{Ae}} = \frac{C_{B0} - C_{A0}X_{Ae}}{C_{A0} - C_{A0}X_{Ae}} = \frac{k_1}{k_2} \tag{8}$$

where 'C_{Ae}' and 'C_{Be}' are the equilibrium concentrations of adsorbate in the solution and adsorbent respectively. The plot for the first-order reversible kinetics as shown in Eq. (6) was drawn for the seaweed at different adsorption parameters where linearity relationship was observed. The correlation coefficients R^2, k_r, k_1 and k_2 were calculated using Eqs. (6) and (8) for different plots and are shown in Table 3.

3.8.3. Ritchie's second-order kinetic model

Ritchie second-order equation can be expressed as

$$\frac{q_e}{q_e - q_t} = 1 + k_2 t \tag{9}$$

where q_t = uptake (mg/g) at time 't', q_e = equilibrium uptake capacity and k_2 = rate constant have their usual meanings. Ritchie second-order equation (Eq. (9)) was fitted to the experimental data. The estimated values of the kinetic model parameters are reported along with correlation coefficient R^2 in Table 3.

3.8.4. Pseudo second-order kinetic model

A pseudo second-order reaction model can also be applicable to the kinetics of sorption and the equation for this reaction can be shown as:

$$\frac{dq}{dt} = k(q_e - q)^2 \tag{10}$$

On integration for boundary conditions when $t = 0$ to $t > 0$ and $q = 0$ to $q > 0$ and further simplifications, Eq. (9) becomes

$$\frac{t}{q} = \frac{1}{kq_e^2} + \frac{1}{q_e}t = \frac{1}{h} + \frac{1}{q_e}t \tag{11}$$

where $h = kq_e^2$ is known as initial sorption rate where 'k' is rate constant, q_t and q_{eq} are the uptake at time t and at equilibrium respectively. The values of k_2 were calculated from the graphs between t/q_t vs. t/q_e. The estimated values of kinetic model parameters along with correlation coefficient R^2 were calculated and are reported in Table 3. From Table 3 it can be concluded that the kinetics followed pseudo second-order model.

3.9. Rate controlling mechanism

The adsorption of Cr(VI) on porous adsorbent can be governed by four consecutive steps such as diffusion in the bulk solution, diffusion across the thin film surrounding the adsorbent particles followed by intra-particle diffusion and desorption within the particles. Any of the above steps or combinations of them may control the rate. To determine the exact mechanism, it is necessary to carry out experiments for pore/solid phase diffusion mechanisms. In many cases, intra-particle diffusion for which the mathematical equation (12) is given below, was observed to be the rate-limiting step:

$$q_t = k_{id}t^{1/2} \tag{12}$$

The plot between q_t and $t^{1/2}$ gives the coefficient of intra-particle diffusion (k_{id}) for different adsorption parameters. The values of intra-particle diffusion coefficient (k_{id}) along with the regression coefficient (R^2) for the plot of q vs. $t^{1/2}$ under different adsorption parameters are given in Table 4. Again, from the plot between 't' (time) and percentage adsorption at different adsorption parameters, was found to be non-linear over the entire time range. In that case, more than one step may affect the adsorption process. So the adsorption process can be divided into two distinct steps: the initial curved portion relates to film diffusion (D_1) and the latter linear portion relates to the diffusion within the adsorbent. The equation for 'D_1' and 'D_2' are given by:

$$\frac{q_t}{q_e} = 6\left(\frac{D_1}{\pi a^2}\right)^{1/2} t^{1/2} \tag{13}$$

$$\ln\left(1 - \frac{q_t}{q_e}\right) = \ln\left(\frac{6}{\pi^2}\right) - \left(\frac{D_2\pi^2 t}{a^2}\right) \tag{14}$$

The values of 'D_1' along with the R^2 under different adsorption parameters were calculated from the slope of the plot between q_t/q_e and $t^{1/2}$ for the initial curved portion and are given in Table 4. Similarly, 'D_2' values were calculated from the slope of the curve between $\ln(1 - q_t/q_e)$ and 't' under different adsorption parameters and are given in Table 4. From Table 4 it is observed that the D_1 values are always less than that of the D_2 values. So it can be concluded that the surface diffusion is the rate controlling mechanism, as it is the slowest rate.

Table 3
Adsorption kinetics model parameters.

Parameters	First-order reversible					Pseudo first-order reversible		Ritchie second-order		Pseudo second-order reversible	
	k_r	K_C	k_1	k_2	R^2	k	R^2	k_2	R^2	k_2	R^2
Stirring speed (rpm)											
200	0.0093	0.75	0.0040	0.0053	0.948	0.0092	0.948	0.0704	0.791	0.0031	0.996
300	0.0108	1.11	0.0057	0.0051	0.972	0.0108	0.972	0.1008	0.819	0.0024	0.996
400	0.0115	1.38	0.0067	0.0048	0.971	0.0115	0.971	0.1278	0.788	0.0023	0.996
500	0.0128	1.72	0.0081	0.0047	0.976	0.0127	0.976	0.1967	0.696	0.0021	0.996
600	0.0117	2.01	0.0078	0.0039	0.982	0.0117	0.982	0.1313	0.789	0.0019	0.995
Initial pH											
2	0.0118	9.12	0.0106	0.0012	0.880	0.0117	0.878	0.2492	0.616	0.0044	0.999
3	0.0136	2.01	0.0091	0.0045	0.920	0.0136	0.919	0.3203	0.529	0.0069	0.995
4	0.0088	0.49	0.0029	0.0059	0.860	0.0088	0.862	0.0710	0.799	0.0020	0.998
5	0.0105	0.33	0.0026	0.0079	0.942	2.4456	0.942	0.0946	0.804	0.0056	0.998
Adsorbate concentration (mg/L)											
100	0.0115	2.013	0.0077	0.0038	0.97	0.0113	0.970	0.1232	0.789	0.0020	0.9953
150	0.0104	0.897	0.0049	0.0055	0.97	0.0104	0.970	0.0624	0.764	0.0015	0.9910
200	0.0098	0.575	0.0036	0.0062	0.95	0.0097	0.950	0.0854	0.773	0.0015	0.9901
250	0.0080	0.425	0.0024	0.0056	0.85	0.0069	0.904	0.1284	0.679	0.0014	0.9910
Adsorbent dose (g/L)											
0.8	0.0101	1.5340	0.0061	0.0040	0.98	0.0101	0.980	0.0688	0.830	0.0007	0.992
1.2	0.0114	1.7073	0.0072	0.0042	0.96	0.0113	0.960	0.1333	0.652	0.0011	0.992
1.6	0.0112	1.8552	0.0073	0.0039	0.98	0.0113	0.980	0.1047	0.815	0.0015	0.995
2	0.0116	2.0126	0.0077	0.0039	0.98	0.0115	0.980	0.1234	0.789	0.0019	0.995
2.4	0.0128	1.7064	0.0081	0.0047	0.95	0.0113	0.950	0.0250	0.988	0.0034	0.996
Temperature (°C)											
27	0.0117	2.0126	0.0078	0.0039	0.982	0.0117	0.98	0.5336	0.976	0.0019	0.995
35	0.0099	2.8333	0.0073	0.0026	0.970	0.0099	0.97	0.8177	0.999	0.0019	0.995
40	0.0107	4.0455	0.0086	0.0021	0.969	0.0108	0.97	1.6706	0.966	0.0019	0.995
45	0.0123	5.7500	0.0105	0.0018	0.959	0.0124	0.96	1.7448	0.967	0.0018	0.994
50	0.0124	12.0000	0.0114	0.0010	0.960	0.0124	0.97	0.2096	0.638	0.0017	0.994

Table 4
Mass transfer model parameters.

Parameters	k_{id}	R^2	$D_1{*}10^{-12}$	R^2	$D_2{*}10^{-12}$	R^2
Stirring (rpm)						
200	0.7617	0.999	0.4974	0.988	0.6252	0.956
300	0.8592	0.980	0.5098	0.973	0.7270	0.987
400	0.8693	0.970	0.5882	0.987	0.7851	0.986
500	0.9677	0.953	0.5489	0.986	0.9378	0.974
600	1.0257	0.956	0.4328	0.981	0.8215	0.989
pH						
1.8	0.5313	0.910	0.5762	0.897	0.7052	0.978
2	0.5868	0.955	0.6906	0.832	0.7342	0.828
3	0.9842	0.984	0.5246	0.988	1.1123	0.845
4	0.9716	0.972	0.6214	0.923	0.5089	0.894
5	0.9799	0.980	58.2183	0.965	0.6325	0.944
Adsorbate concentration (mg/L)						
50	0.3498	0.9405	0.4122	0.995	0.8360	0.904
100	1.0289	0.9626	0.5246	0.978	0.8215	0.988
150	1.4652	0.9827	0.2899	0.971	0.7851	0.983
200	1.5641	0.9836	0.3640	0.948	0.7415	0.956
250	1.261	0.9891	0.5690	0.984	0.5598	0.961
Adsorbent dose (g/L)						
0.8	2.3618	0.991	0.5762	0.990	0.6979	0.973
1.2	1.7201	0.9992	0.4338	0.965	0.8506	0.924
1.6	1.3588	0.9773	0.3931	0.979	0.7706	0.991
2	1.1326	0.976	0.4235	0.981	0.8215	0.978
2.4	0.8437	0.9888	0.2934	0.845	1.0541	0.939
Temperature (°C)						
27	1.1364	0.972	0.4235	0.981	0.8215	0.989
35	1.1541	0.981	0.4061	0.985	0.6470	0.984
40	1.2101	0.995	0.3902	0.984	0.7561	0.964
45	1.3164	0.992	0.3991	0.985	0.9596	0.931
50	1.3343	0.995	0.3322	0.988	0.9669	0.931

3.10. Adsorption isotherm study

An adsorption isotherm can be utilized to obtain information concerning the desorption mechanism strictly connected with interaction between the adsorbent and adsorbate molecules. Therefore, the efficiency of an industrial adsorbent can be assessed through an adsorption isotherm curve. The adsorption isotherm thus developed provides useful information for estimating performance in a full-scale process stream. Firstly, they help to determine the possibility to reach a desired purity level for a given adsorbent. Secondly, the isotherm allows calculation of uptake (q_e) at equilibrium, which has a major impact on the process economy. It can also be used to predict the relative performance of different types of adsorbents. A number of isotherm equations were proposed by different investigators. Some of those in frequent use are:

- Freundlich adsorption isotherm.
- Langmuir adsorption isotherm.
- Temkin adsorption isotherm.

3.10.1. Freundlich isotherm

The Freundlich adsorption equation can be written as:

$$\frac{x}{m} = q_e = kc^{1/n} \tag{15}$$

Taking the logarithm of both sides,

$$\log q_e = \log k + \frac{1}{n} \log C_e = K_f + \frac{1}{n} \log C_e \tag{16}$$

where 'q_e' is equilibrium adsorption capacity (mg/g), 'C_e' is the equilibrium concentration of the adsorbate in solution, 'K_f', and 'n' are constants related to the adsorption process such as adsorption capacity and intensity respectively.

3.10.2. Langmuir adsorption isotherm

The Langmuir equation is given by:

$$\frac{C_e}{q_e} = \frac{1}{Q_0 b} + \frac{C_e}{Q_0} \quad (17)$$

where 'C_e' is the equilibrium concentration and 'q_e' is the amount of adsorbate adsorbed per gram of adsorbent at equilibrium (mg/g); 'Q_0' and 'b' are Langmuir constants related to the sorption capacity and intensity respectively.

3.10.3. Temkin adsorption isotherm

Temkin and Pyzhev suggested that due to the indirect adsorbate/adsorbent interaction, the heat of adsorption of all the molecules in the layer would decrease linearly with coverage. The linear form of Temkin isotherm can be written as:

$$q_{eq} = B \ln A + B \ln C_{eq} \quad (18)$$

where $B = RT/b$, 'T' is temperature in Kelvin and 'R' is the universal gas constant. The constant 'b' is related to heat of adsorption, C_{eq} = equilibrium concentration of the adsorbate. Langmuir constants Q_0, b; Frendluich constants h_f, b_f and Temkin constants A, B were calculated from the plots between C_e/q_e vs. C_e, $\ln q_e$ vs. $\ln C_e$ and q_e vs. C_e respectively. The estimated values of the model parameters are reported in Table 4 along with other statistical parameters such as correlation coefficient (R^2) and the average absolute percentage deviation between $q_{e(\text{cal})}$ and $q_{e(\text{exp})}$. It can be concluded from Table 5 that the experimental data were well fit to the Langmuir adsorption isotherm model. Almost all b_f values were in the range of 0.01–1 indicating the adsorption to be favorable.

3.11. Statistical design of experiments

In order to develop an adsorption process, a number of influencing parameters such as contact time, pH, adsorbate concentration, adsorbent dose, stirring speed, particle size and temperature are to be studied. But the process of studying each and every variance separately is quite tedious as well as time consuming. Further, conventional and classical methods of studying the effect of different factors involved in the adsorption process at an unspecified constant level do not depict the combined effect of all the factors involved [44]. Again, this method requires a large number of experiments to determine the optimal levels, which are unreliable. Thus, the optimization of all the affecting parameters collectively by using a designed experimental model can minimize the above difficulties [45,46]. Experimental design method is an important tool in engineering science for improving the performance of the process. Further, the design of experiment determines which factors have important effects on a response as well as how the effect of one factor varies with the level of the other factors [47–50]. In addition, a factorial experiment is the only source to make it possible to quantitatively assess the individual independent term as well as interaction effects of different coefficients and factors.

A full factorial design of the type n^k was used in the present study to find out the optimum conditions for adsorption of Cr(VI) on the seaweed, where 'n' is the number of levels and 'k' is number of factors under verification. Here time, pH, adsorbent dose and adsorbent concentration are chosen as four independent factors or variables ($k = 4$ and $n = 2$) and the Cr(VI) loading of adsorption as the dependent out-put response variable. A 2^4 full-factorial experimental design [49] with 3 triplicates at the center point, and thus a total of 20 experiments were employed in this study. The base levels or the average of two level are calculated for statistical calculation

Table 5
Adsorption isotherm parameters.

Parameter	Langmuir adsorption isotherm						Freundlich adsorption isotherm					Temkin adsorption isotherm				
	Q_0	b	R^2	$q_{e,\text{exp}}$	$q_{e,\text{cal}}$	%Desv	b_f	k_f	R^2	$q_{e,\text{cal}}$	%Desv	A	b	R^2	$q_{e,\text{cal}}$	%Desv
Stirring speed (rpm)																
200	23.98	0.12	0.99	30.00	30.60	0.35	0.41	139.60	0.98	30.54	1.36	332.19	173.50	0.99	30.43	0.97
300				34.45	33.22					33.87					34.05	
400				36.70	35.54					36.13					36.30	
500				38.75	38.96					38.71					38.70	
600				40.05	42.43					40.72					40.47	
Initial pH																
1.8	20.41	0.26	0.96	50.00	50.00	6.80	0.34	90.76	0.87	50.00	8.92	471.22	226.03	0.92	67.92	8.21
2				47.40	81.00					51.91					49.73	
3				40.05	25.37					32.94					34.92	
4				24.75	22.11					24.02					24.65	
5				19.75	21.81					22.60					22.65	
Adsorbate concentration (mg/L)																
50	56.82	0.19	0.99	25.00	25.00	3.46	0.17	23.87	0.99	25.00	0.78	6.36	301.15	1.00	15.33	0.60
100				40.05	44.69					40.27					40.10	
150				48.15	51.63					47.90					48.32	
200				53.50	53.70					52.73					52.87	
250				55.75	54.69					56.54					56.17	
Adsorbent dose (g/L)																
0.8	196.08	0.01	0.99	68.88	69.10	0.21	0.75	4.09	0.98	70.18	3.29	66.78	7.17	0.99	68.49	2.26
1.2				56.00	55.77					55.50					56.76	
1.6				46.75	45.87					45.58					46.92	
2				40.05	38.10					38.20					38.10	
2.4				33.96	35.91					36.18					35.37	
Temperature (°C)																
27	38.46	0.85	1.00	40.05	40.87	1.67	0.11	56.78	0.93	40.97	1.59	97525.50	517.65	0.94	40.94	1.42
35				42.50	41.72					42.26					42.30	
40				44.50	43.05					43.71					43.80	
45				46.00	45.07					45.26					45.33	
50				48.00	54.42					48.81					48.67	

Table 6
Factorial levels and variation intervals.

Factors	−1	0	1	Variation interval
x_1	20	30	40	10
x_2	2	3	4	1
x_3	1.6	2.0	2.4	0.4
$x4$	50	100	150	50

x_1 = Time in min, x_2 = pH, x_3 = adsorbent dose in °C, x_4 = adsorbate concentration (mg/L).

using the following relation:

$$x_i = \frac{(X_i - X_0)}{\delta X} \tag{19}$$

The behavior of the system was explained by the following equation:

$$Y = b_0 + b_1x_1 + b_2x_2 + b_3x_3 + b_4x_4 + b_{12}x_1x_2 + b_{23}x_2x_3 + b_{31}x_3x_1 + b_{14}x_1x_4 + b_{24}x_2x_4 + b_{34}x_3x_4 + b_{123}x_1x_2x_3 + b_{124}x_1x_2x_4 + b_{134}x_1x_3x_4 + b_{234}x_2x_3x_4 + b_{1234}x_1x_2x_3x_4 \tag{20}$$

where b_0, $b_1, \ldots, b_{123}$ are the regression interaction coefficients of the concerned variables and x_1, x_2 and x_3 are the dimensionless coded factors affecting the process; x_1 = time, x_2 = pH, x_3 = adsorbent dose and x_4 = adsorbate concentration. The factorial levels and variation intervals of the coded factor are shown in Table 6.

The parameters varied were time (20–40 min), pH (2–4), adsorbate concentration (50–150 mg/L) and adsorbent dose (1.6–2.4 g/L). The variable parameters in two levels, their coded values and the conditions for the base level experiments are given in Table 7. The +, − and 0 designations are given to the higher, lower and base levels respectively. The coefficients were calculated using the following equation:

$$b_j = \frac{\left(\sum X_{ij}Y_j\right)}{N} \tag{21}$$

where $j = 1, 2, 3, 4, \ldots, n$ and 'i' and 'j' are the number of rows and columns respectively. The results obtained from trial runs are incorporated in the regression equation and thus the equation becomes:

$$Y = 38.5 + 3.44x_1 - 24.06x_2 + 2.19x_3 - 8.44x_4 + 0.31x_1x_2 - 3.44x_2x_3 + 0.31x_3x_1 + 0.94x_1x_4 + 0.94x_2x_4 - 0.31x_3x_4 + 0.9375x_1x_2x_3 - 3.43x_1x_2x_4 - 0.94x_1x_3x_4 + 2.81x_2x_3x_4 + 3.44x_1x_2x_3x_4 \tag{22}$$

The significance of each coefficient was assessed using the Student's 't'-test [51] and the insignificant terms were neglected from equation (22). Fisher's adequacy test [52] at 99% confidence level was used to test the regression equation and it was observed that the following equation was adequate:

$$Y = 38.5 + 3.44x_1 - 24.06x_2 + 2.19x_3 - 8.44x_4 - 3.44x_2x_3 - 3.43x_1x_2x_4 + 2.81x_2x_3x_4 + 3.44x_1x_2x_3x_4 \tag{23}$$

From Eq. (23) it can be seen that the coefficient of 'x_2' is found to be the largest negative value, which implies that the pH has the most influential effect on the adsorption process and the percentage adsorption decreased with increase in pH. Similarly it can be observed that the adsorbate concentration is the second most influential factor followed by time and the combined effect of the four variables. The adsorbent dose has the least influence on the adsorption process.

3.12. Multi-variate analysis

Multi-variate analysis technique was used to correlate the different adsorption parameters. 10 variables were considered in all. Some of the variables were measured directly and some were calculated from the measured values. Table 8 shows the correlation matrix. The reaction time showed good correlation with different adsorption kinetic parameters like pH, % adsorption, uptake of Cr values from aqueous phase as well as the rate of adsorption. pH showed a negative correlation with adsorption rate indicating increase of pH would have a negative effect on the adsorption efficiency.

Elements belonging to a given factor were defined by factorial matrix after varimax rotation, with those having strong correlation grouped into factors (Table 9). For multivariate analysis, the eigen values up to 1 was considered since the results with eigen values beyond 1 were not very significant. Based on these, all variables were classified into two groups as shown below:

(a) Factors related to adsorption kinetics.
(b) Factors 2–4 related to adsorption parameters.

Factor-1: exhibit 33.8% of the total variance of 75.3%. In this Factor, most of the major variables (5 numbers) were included. Factor loading values of 0.5 were considered for $p < 0.05$ [53]. This fac-

Table 7
Design of trial runs (in coded form) for adsorption of Cr (VI).

Trial no.	x_1	x_2	x_3	x_4	x_1x_2	x_1x_3	x_1x_4	x_2x_3	x_2x_4	x_3x_4	$x_1x_2x_3$	$x_1x_2x_4$	$x_1x_3x_4$	$x_2x_3x_4$	$x_1x_2x_3x_4$	Y
1	+	+	+	+	+	+	+	+	+	+	+	+	+	+	+	25
2	+	+	+	−	+	+	−	+	−	−	+	−	−	−	−	35
3	+	+	−	+	+	−	+	−	+	−	−	+	−	−	−	15
4	+	−	+	+	−	+	+	−	−	+	−	−	+	−	−	70
5	−	+	+	+	−	−	−	+	+	+	−	−	−	+	−	15
6	+	+	−	−	+	−	−	−	−	+	−	−	+	+	+	45
7	+	−	−	+	−	−	+	+	−	−	+	−	−	+	+	75
8	+	−	+	−	−	+	−	−	+	−	−	+	−	+	+	95
9	−	+	+	−	−	−	+	+	−	−	−	+	+	−	+	25
10	−	+	−	+	−	+	−	−	+	−	+	−	+	−	+	20
11	−	−	+	+	+	−	−	−	−	+	+	+	−	−	+	65
12	+	−	−	−	−	−	−	+	+	+	+	+	+	−	−	70
13	−	+	−	−	−	+	+	−	−	+	+	+	−	+	−	30
14	−	−	+	−	+	−	+	−	+	−	+	−	+	+	−	90
15	−	−	−	+	+	+	−	+	−	−	−	+	+	+	−	50
16	−	−	−	−	+	+	+	+	+	+	−	−	−	−	+	80
17	0	0	0	0	0	0	0	0	0	0	0	0	0	0	0	38
18	0	0	0	0	0	0	0	0	0	0	0	0	0	0	0	37.1
19	0	0	0	0	0	0	0	0	0	0	0	0	0	0	0	39.2
20	0	0	0	0	0	0	0	0	0	0	0	0	0	0	0	38.5

Table 8
Correlation matrix showing the inter-relation between the variables (bold letter indicates $p < 0.001$).

	Time	pH	Adsorbate concentration	Adsorbent dose	Stirring speed	Temperature	% adsorption	Loading	Concentration	Rate of adsorption
Time	1.000									
pH	**0.428**	1.000								
Adsorbate	0.000	0.028	1.000							
Adsorbent	0.008	−0.016	0.089	1.000						
Stirring speed	0.000	−0.041	0.128	−0.132	1.000					
Temperature	0.000	0.042	−0.132	0.137	0.196	1.000				
% ads	**0.669**	0.211	−0.266	0.198	0.096	0.175	1.000			
Loading	**0.704**	0.284	0.192	−0.164	0.174	0.057	**0.749**	1.000		
Conc.	**−0.445**	−0.137	**0.779**	−0.056	0.036	−0.201	**−0.784**	**−0.399**	1.000	
Rate of adso., mg/g/min	**−0.403**	**−0.472**	0.048	−0.007	0.070	0.000	**−0.345**	**−0.348**	0.261	1.000

Table 9
VARIMAX rotated component analysis Factor matrix.

	Component			
	1	2	3	4
Time	0.812			
pH				
Adsorbate		0.863		
Adsorbent				0.919
Stirring speed			0.806	
Temperature			0.509	
% ads	0.908			
Loading	.777			
Conc.	−0.786	0.593		
Rate of adsorption, mg/g/min	−0.567			
Eigen values	Cumulative variance			
3.38	33.8			
1.71	50.9			
1.29	63.8			
1.15	75.3			

tor includes all variables related to determination of adsorption kinetics.

Factors 2–4: exhibit 42.5% of variance. These three factors constitute all adsorption parameters like adsorbate and adsorbent concentration, stirring speed and temperature.

The adsorption capacity of the present adsorbent was compared with other similar adsorbents for Cr(VI) reported in literature. The comparison is shown in Table 10, from which it can be concluded that the present adsorbent is efficient in treating Cr(VI) contaminated water.

Table 10
Comparison of adsorption parameters and uptake capacity with other reported adsorbents.

Adsorbent	Uptake capacity	pH	Initial conc. (mg/L)	Reference
Chlorella vulgaris	24	2	25–250	[55]
Zooglera ramigera	3	2	25–400	[55]
Halimeda opuntia	40	4.1	25–400	[55]
Rhizopaus arrhizus	62	2	25–400	[56]
Rhizopaus arrhizus	8.8	2		[55]
Sargassum	40	2		[57]
Spirogira	14.7	2	25 Jan	[58]
Tyres activated carbon	58.50	2	60	[59]
Coconut shell carbon	20	2	–	[60]
Coconut shell carbon	10.88	4	25	[61]
Sawdust activated carbon	44.05	2	200	[22]
Hydrilla verticillata	247	3	100	Current study

4. Conclusion

The seaweed used in this study for the removal of Cr(VI) from waste water is easily available and can be processed to get a low cost adsorbent. Feasibility of the adsorption process was studied in batch scale. Effects of different adsorption parameters on the adsorption process were studied. From the FTIR analysis, it was observed that the high adsorption capacity of the adsorbent is due to the presence of different surface functional groups such as carboxyl and amine groups, in the adsorbent. These groups react with the Cr(VI) species present in the aqueous solution. Experimental adsorption data followed pseudo second-order kinetics. Among the different adsorption isotherms, Langmuir adsorption isotherm is best fit to the experimental data. Intra-particle diffusion was found to be the rate limiting step. Different thermodynamic parameters were evaluated for the Cr(VI) adsorption process. Statistical analysis showed that pH has the most influential effect and adsorbent dose has the least influential effect on the adsorption process. The correlation between different adsorption parameters in the process was evaluated using multivariate analysis.

Acknowledgements

The authors are thankful to the Director, Birla Institute of Technology and Science, Pilani – Goa Campus for giving permission to publish the work. The authors are also thankful to the Director, Institute of Minerals and Materials Technology (CSIR), Bhubaneswar for providing the experimental facility to carry out the work. One of the authors, Namrata Das, is thankful to the Council of Scientific and Industrial Research, Extra-mural Division for providing fellowship.

References

[1] A.J.M. Barros, S. Prasad, V.D. Leite, A.V. Souza, Biosorption of heavy metal in up flow sludge columns, Bioresour. Technol. 98 (2007) 1418–1425.
[2] D.C. Sarma, S.C. Malhotra, Chromium toxicity effect on wheat, Indian J. Environ. HITH 35 (1993) 47–49.
[3] M. Costa, Potential hazards of hexavalent chromate in our drinking water, Toxicol. Appl. Pharm. 188 (2003) 1–5.
[4] S.A. Katz, S. Salem, The toxicity of chromium with respect to its chemical speciation: a review, J. Appl. Toxicol. 13 (2006) 217–224.
[5] S.S. Baral, S.N. Das, P. Rath, G. Roy Chaudhury, Chromium (VI) removal by calcined bauxite, Biochem. Eng. J. 34 (2007) 69–75.
[6] S.S. Baral, S.N. Das, P. Rath, G. Roy Chaudhury, Y.V. Swamy, Removal of Cr(VI) from aqueous solution using waste weed, *Salvinia cucullata*, Chem. Ecol. 23 (2007) 105–117.
[7] N. Sapari, A. Idris, N. Hisham, A. Hamid, Total removal of heavy metal from mixed plating rinse wastewater, Desalination 106 (1996) 419–422.
[8] S.M. Corvalan, I. Ortiz, A.M. Eliceche, Optimal design of membrane process for wastewater treatment and metal recovery, Comput. Chem. Eng. 28 (2004) 103–109.
[9] S.N. Das, Final Report on Abatement of Pollution due to Chromite Mining in Orissa—Phase-II, Treatment of Mine Water, 1999.
[10] J.W. Patterson, Water Treatment Technology, 3rd ed., Ann Arbor Science, Ann Arbor Michigan, MI, 1998.

[11] B. Mukhopadhyay, J. Sundquist, R.J. Schmitz, Removal of Cr(VI) from chromium contaminated ground water through electrochemical addition of Fe(II), J. Environ. Manage. 82 (2007) 66–76.
[12] G. Arslan, E. Pehlivan, Batch removal of Cr(VI) from aqueous solution by Turkish brown coals, Bioresour. Technol. 98 (2007) 2836–2845.
[13] H. Li, T. Liu, Z. Li, L. Deng, Low-cost supports used to immobilize fungi and reliable technique for removal hexavalent chromium in wastewater, Bioresour. Technol. 99 (2008) 6271–6279.
[14] V.K. Garg, R. Gupta, R. Kumar, R.K. Gupta, Adsorption of Cr from aqueous solution on treated saw dust, Bioresour. Technol. 92 (2004) 78–81.
[15] B. Preetha, T. Viruthagiri, Batch and continuous bisorption of chromium(VI) by *Rhizopuc arrhizus*, Sep. Purif. Technol. 57 (2007) 126–133.
[16] M.X. Loukidou, A.I. Zouboulis, T.D. Karapantsios, K.A. Matis, Equilibrium and kinetic modeling of chromium(VI) biosorption by *Aeromonas caviae*, Colloids Surf. A: Physicochem. Eng. Aspects 242 (2004) 93–104.
[17] D. Park, S.R. Lim, Y.S. Yun, J.M. Park, Reliable evidences that the removal mechanism of hexavalent chromium by natural biomaterials is adsorption-coupled reduction, Chemosphere 70 (2007) 298–305.
[18] S.E. Bailey, T.J. Olin, R.N. Bricka, D.D. Adrian, A review on potential low cost sorbent for heavy metals, Water Res. 33 (1999) 2469–2479.
[19] L. Chun, C. Hongzhang, M.L. Zuohu, Adsorptive removal of Cr (VI) be Fe-modified steam exploded wheat straw, Process Biochem. 39 (2004) 541–545.
[20] E. Malkoc, Y. Nuhoglu, M. Dundar, Adsorption of chromium(VI) on pomace—an olive oil industry waste: batch and column studies, J. Hazard. Mater. B138 (2006) 142–151.
[21] G. McKay, Use of Adsorbents for the Removal of Pollutants from Wastewaters, CRC Press, Boca Raton, NY, 1995.
[22] T. Karthikeyen, S. Rajgpal, L.R. Miranda, Cr(VI) adsorption from aqueous solution by *Hevea brasilinesis* saw dust activated carbon, J. Hazard. Mater. 124 (2005) 192–199.
[23] D. Park, Y.S. Yun, J.M. Park, Reduction of hexavalent chromium with the brown seaweed *Ecklonia* biomass, Environ. Sci. Technol. 38 (2004) 4860–4864.
[24] Z.R. Holan, B. Volesky, Biosorption of lead and nickel by biomass of marine algae, Biotechnol. Bioeng. 43 (1994) 1001–1009.
[25] E. Fourest, C. Canal, J.C. Roux, Improvement of heavy metal biosorption by mycelial dead biomasses (*Rhizopus arrhizus*, *Muchor miehei*, and *Pencillium chrysogenum*): pH control, and cationic activation, FEMS Microbiol. Rev. 14 (1994) 325–332.
[26] J.T. Matheickal, Q. Yu, Biosorption of lead from aqueous solutions by marine alga *Ecklonia radiate*, Water Sci. Technol. 34 (1996) 1–7.
[27] R.H. Crist, J.R.J. Martin, D.R. Chonko, Crist, Uptake of metals on peat moss: an ion exchange process, Environ. Sci. Technol. 30 (1996) 2456–2461.
[28] F.N. Acar, E. Malkoc, The removal of chromium(VI) from aqueous solutions by *Fagus orientalis* L., Bioresour. Technol. 94 (2004) 13–15.
[29] E. Malkoc, Y. Nuhoglu, The removal of chromium(VI) from synthetic wastewater by *Ulothrix zonata*, Fresen. Environ. Bull. 12 (2003) 376–381.
[30] D. Park, S.Y. Yun, J.M. Park, Studies on hexavalent chromium biosorption by chemically treated biomass of *Ecklonia* sp., Chemosphere 60 (2005) 1356–1364.
[31] Y. Nuhoglu, E. Oguz, Removal of copper(II) from aqueous solutions by biosorption on the cone biomas of *Thuja orientalis*, Process Biochem. 38 (2003) 1627–1631.
[32] J.C. Bailar Jr., H.J. Emeleus, R. Nyholm, A.F. Trotman-Dickenson, Comprehensive Inorganic Chemistry, vol. 3, Pergamon, 1973, p. 693.
[33] N. Tewari, P. Vasudevan, B.K. Guha, Study on biosorption of Cr(VI) by *Mucor hiemalis*, Biochem. Eng. J. 23 (2005) 185–192.
[34] A. Mehrotra, K. Gopal, P.K. Seth, Annual Report VIO Hyderabad State Indian Council of Agriculture Research, ICAR, New Delhi, 1999.
[35] V. Sarin, K.K. Pant, Removal of chromium from industrial waste by using eucalyptus bark, Bioresour. Technol. 97 (2006) 15–20.
[36] M.K. Donais, R. Henry, T. Rettberg, Chromium speciation using an automated liquid handling system with inductively coupled plasma-mass spectrometric detection, Talanta 49 (1999) 1045–1050.
[37] R. Biesuz, M. Pesavento, A. Gonzalo, M. Valiente, Sorption of proton and heavy metal ions on a macroporous chelating resin with an iminodiacetate active group as a function of temperature, Talanta 47 (1997) 127–136.
[38] P. Jones, P.N. Nesterenko, High-performance chelation ion chromatography: a new dimension in the separation and determination of trace metals, J. Chromatogr. A 789 (1997) 413–435.
[39] R.S. Juang, L.D. Shiau, Ion exchange equilibria of metal chelates of ethylenediamine tetraacetic acid (EDTA) with amberlite IRA-68, Ind. Eng. Chem. 37 (1998) 555–560.
[40] D.O. Cooney, Adsorption Design for Wastewater Treatment, Lewis Publishers, London, 1999, pp. 1–87.
[41] C. Raji, T.S. Anirudhan, Batch Cr(VI) removal by polyacrylamide grafted sawdust: kinetics and thermodynamics, Water Res. 32 (1998) 3772–3780.
[42] K. Kadirvelu, K. Thamaraiselvi, C. Namasivayam, Adsorption of nickel(II) from aqueous solution onto activated carbon prepared from coirpith, Sep. Purif. Technol. 24 (2001) 497–505.
[43] R. Leyva-Ramos, A. Juarez-Martinez, R.M. Guerrero-Coronado, Adsorption of chromium(VI) from aqueous solutions on activated carbon, Water Sci. Technol. 30 (1994) 191–197.
[44] K. Ravikumar, K. Pakshirajan, T. Swaminathan, K. Balu, Optimization of batch process parameters using response surface methodology for dye removal by novel adsorbent, Chem. Eng. J. 105 (2005) 131–138.
[45] M. Elibol, Response surface methodological approach for inclusion of perfluorocarbon in actinorhodin fermentation medium, Process Biochem. 38 (2002) 667–673.
[46] A.M. Gun, M.K. Gupta, B. Dasgupta, Designs of Experiments, Fundamental of Statistic, vol. 2, 7th ed., The World Press Private Ltd., Calcutta, 2002, pp. 62–164.
[47] D.C. Montgomery, Design, Analysis of Experiments, 5th ed., John Wiley and Sons, New York, 2001.
[48] G.E.P. Box, W.G. Hunter, J.S. Hunter, Statistics for Experimenters—An Introduction to Design, Data Analysis and Model Building, John Wiley and Sons, New York, 1978.
[49] L.T. Arenas, E.C. Lima, A.A.D. Santos, J.C.P. Vaghetti, T.M.H. Coasta, E.V. Benvenutti, Use of statistical design of experiments to evaluate the sorption capacity of 1,4-diazoniabicycle[2.2.2]octane/silica chloride for Cr(VI) adsorption, Colloids Surf. A: Physiochem. Eng. Aspects 297 (2006) 240–248.
[50] The Statistic homepage, http://www.statsoft.com/textbook/stathome.html, Experimental Design link, website visited on May 26, 2006.
[51] S. Devy, R. Bai, Removal of trivalent and hexavalent chromium with aminated polyacrylonitrile fibers: performance and mechanism, Water Res. 38 (2004) 2424–2432.
[52] S. Akhnazarova, V. Katarov, Experimental Optimization in Chemistry and Chemical Engineering, vols. 151–161, MIR Publisher, Mosco, 1982, pp. 300–330.
[53] J.F. Hair, R.E. Anderson, R.L. Tatham, W.C. Black, Multivariate Data Analysis, Prentice Hall Int, New Jersey, 1998.
[54] V.M. Boddu, K. Abburi, J.L.E.D. Talbott Smith, Removal of hexavalent chromium from wastewater using a new composite chitosan biosorbent, Environ. Sci. Technol. 37 (2003) 4449–4456.
[55] F. Veglio, F. Beolcini, Removal of metals by biosorption: a review, Hydrometallurgy 44 (1997) 301.
[56] S. Prakasan, J.S. Merre, R. Sheela, N. Saswati, S. Ramakrisna, Biosorption of chromium VI by free and immobilized *Rhizopus arrhizus*, Environ. Pollut. 104 (1999) 421.
[57] D. Kratochvil, P. Pimentel, B. Volesky, Removal of trivalent and hexavalent chromium by seaweed biosorbent, Environ. Sci. Technol. 32 (1998) 2693.
[58] D. Kratochvil, P. Pimentel, Advances in the biosorption of heavy metals, Trends Biotechnol. 16 (1998) 291.
[59] N.K. Hamadi, X.D. Chen, M.M. Farid, M.G.Q. Lu, Adsorption kinetics for the removal of chromium(VI) from aqueous solution by adsorbents derived from used tyres and sawdust, Chem. Eng. J. 84 (2001) 95–105.
[60] G.J. Alaerts, V. Jitjaturant, P. Kelderman, Use of coconut shell based activated carbon for chromium(VI) removal, Water Sci. Technol. 21 (1989) 1701–1704.
[61] S. Babel, T.A. Kurniawan, Cr(VI) removal from synthetic wastewater using coconut shell charcoal and commercial activated carbon modified with oxidizing agents and/or chitosan, Chemosphere 54 (2000) 951–967.